IOP PUBLISHING PHYSICS IN MEDICINE AND BIOLOGY

Phys. Med. Biol. **53** (2008) 4203–4212 doi:10.1088/0031-9155/53/15/013

Noninvasive photoacoustic imaging of the developing vasculature during early tumor growth

Yeqi Lao, Da Xing, Sihua Yang and Liangzhong Xiang

MOE Key Laboratory of Laser Life Science, South China Normal University, Guangzhou 510631, People's Republic of China
and
Institute of Laser Life Science, South China Normal University, Guangzhou 510631, People's Republic of China

E-mail: xingda@scnu.edu.cn

Received 6 May 2008, in final form 18 June 2008
Published 17 July 2008
Online at stacks.iop.org/PMB/53/4203

Abstract

In this study, we monitor the progress of vasculature in early tumor growth using photoacoustic imaging over a 20 day period after subcutaneous inoculation of breast cancer tumor cells in a mouse. With 532 nm laser pulses employed as an irradiation source, the photoacoustic images were obtained through the photoacoustic signals received by a hydrophone in orthogonal mode. The morphological characteristics of vasculature in tumor region are clearly resolved in the photoacoustic images, and the change in structure as well as the increase in density can be identified. Moreover, the average photoacoustic signal strength of vasculature in tumor region, which is highly correlated with the total hemoglobin concentration of blood, is enhanced during early tumor growth. These results indicate the feasibility of detecting early stage tumor and monitoring the progress of anti-angiogenic therapy by photoacoustic imaging.

(Some figures in this article are in colour only in the electronic version)

1. Introduction

Tumor angiogenesis is the central part of tumor growth. In contrast to normal vessels, tumor vessels are structurally and functionally abnormal. An understanding of parameters of neovascularization in early tumor growth, such as vessel formation, the architecture and function of the resulting vessels, is therefore important for clinicians who diagnose and treat cancer. Imaging modalities for detecting early stage tumors and monitoring the progress of tumor growth and anti-angiogenic therapy should be noninvasive, resolve the vascular networks in the tumor region with high spatial resolution, and furthermore, be able to realize functional and molecular imaging. The imaging modalities employed nowadays to

assess breast cancer, one of the most common cancers, include x-rays, near-infrared optical imaging, ultrasonography and magnetic resonance imaging. X-rays are invasive to human body, near-infrared optical imaging is limited by its low spatial resolution (Zhu *et al* 2003) and ultrasonography and magnetic resonance imaging often involve extrinsic contrast agents (Krix *et al* 2003, Anderson *et al* 2001). One potential noninvasive imaging modality using intrinsic contrast agents, for instance hemoglobin, is photoacoustic imaging. In this technique, ultrasonic signals (photoacoustic signals) are generated on the basis of optical absorption of the biological tissue. Photoacoustic imaging consists of the advantages of high contrast in optical imaging and high resolution in ultrasound imaging. These features bring a bright future to this technique in the use of detecting breast cancer and other diseases of blood vessels (Khamapirad *et al* 2005, Ermilov *et al* 2006, Xiang *et al* 2007, Yang *et al* 2007a, 2007b). Previously, photoacoustic imaging of tumor angiogenesis in rat brains has been done *in vivo* (Ku *et al* 2005). Due to the limited spatial resolution, previous work on photoacoustic imaging of tumor neovascularization could not show the architectural change and give qualitative analysis of the morphology parameters of the developing vasculature in early tumor growth (Siphanto *et al* 2005).

Here, we present photoacoustic images of the developing vasculature in early tumor growth obtained over a 20 day period after subcutaneous inoculation of breast cancer tumor cells in a mouse. With the photoacoustic signals captured by a hydrophone in orthogonal mode, the morphological characteristics of the developing vasculature in tumor region are clearly resolved through two-dimensional photoacoustic images. A 6 mm $\times$ 9 mm area in the tumor region was selected for the purpose of qualitative analysis of the morphology parameters. In this area, the average photoacoustic signal strength of blood vessel, the average vessel diameter and the vessel density underwent significant changes during early tumor growth.

2. Materials and methods

2.1. Photoacoustic imaging system

The schematic of our photoacoustic imaging system is shown in figure 1. A Q-switched Nd:YAG laser (LOTIS TII Ltd, Minsk, Belarus), operating at the second harmonic wave, was employed as the excitation source to provide 532 nm laser pulses with a full-width half-maximum (FWHM) value of 10 ns and a repetition rate of 15 Hz. The laser beam was expanded and homogenized to illuminate the back of the mouse, controlled to an energy density of $\sim$10 mJ cm^{-2} in all the experiments. A needle polyvinylidene fluoride (PVDF) hydrophone (Precision Acoustics Ltd, Dorchester, UK) with a diameter of 1 mm and a sensitivity of 850 nV Pa^{-1} was used to receive photoacoustic signals. The hydrophone, driven by a computer-controlled step motor to scan around the mouse, completed a full view of a 2π circular scan with 200 steps (1.8°/step). The received photoacoustic signals were amplified and recorded by a digital oscilloscope (TDS3032, Tektronix, USA), and then transmitted to a personal computer for subsequent data processing. A modified filtered backprojection algorithm was used to reconstruct the photoacoustic images (Wang *et al* 2004). The hydrophone was immersed in water for better coupling of photoacoustic signals. The mouse was allowed to protrude into the water tank through a hole at the bottom of the tank and was insulated from the water by a piece of clear polyethylene membrane covering the hole. The mouse and the hydrophone were fixed on a precision three-dimensional translation stage and a homemade holder, respectively. Both the translation stage and the hydrophone can be manually adjusted to align the scanning plane.

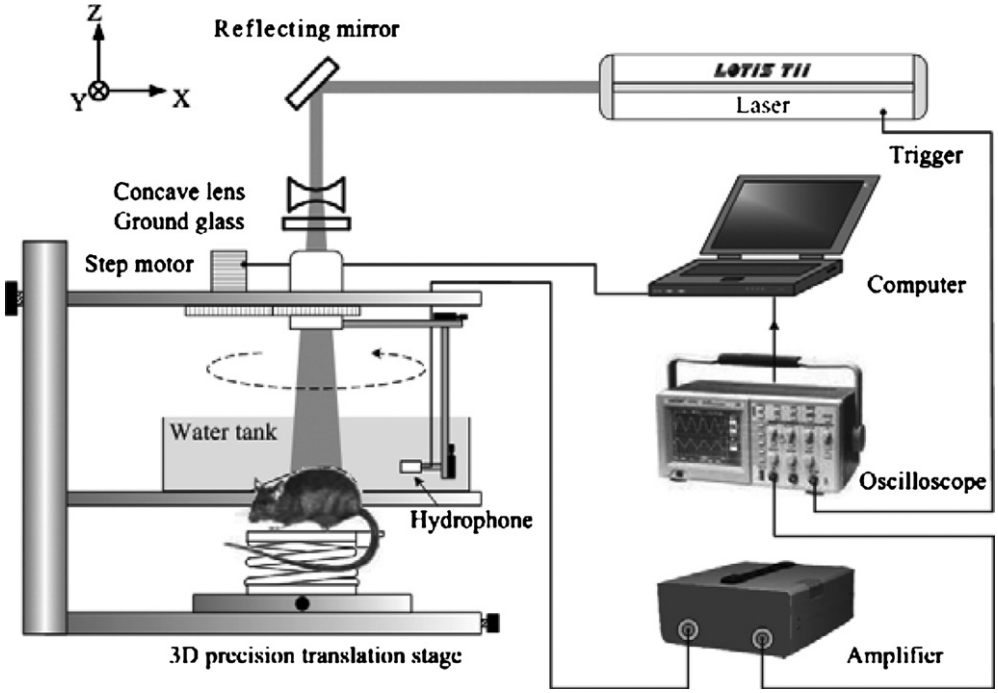

Figure 1. Schematic diagram of the photoacoustic imaging system.

2.2. Animal model

BALB/c mice of ∼20 g body weight and ∼6 weeks age were employed in our experiment. General anesthesia was administered to the mouse by an intraperitoneal injection of pentobarbital. Before photoacoustic imaging, the hair of the imaging area on the mouse was removed gently with a hair-remover lotion to improve light penetration. A sufficient amount of ultrasound gel was applied on the imaging area as an acoustic coupling medium for photoacoustic signals. A mouse tumor model was developed in our experiment. 2×10^6 murine mammary tumor line C127 cells, which were cultured in Dulbecco's modified Eagle's medium (DMEM) supplemented with 15% fetal calf serum (FCS) in 5% CO_2, 95% air at 37 °C in a humidified incubator, were injected under the epidermis on the back of the mouse.

2.3. Localization before photoacoustic imaging

For locating the same spot for serial photoacoustic imaging, the laser beam path was kept constant during the study period. An area of approximately 18 mm × 15 mm around the inoculation site on the mouse was defined by some markers to ensure its illumination by the laser beam throughout the study period. The hydrophone began to circularly receive photoacoustic signals from the same place in the same direction. The locations of the hydrophone fixed on the holder and the mouse fixed on the translation stage as well as the height from the translation stage to the back of the mouse were invariable. Besides, the position of the mouse protruded into the water tank was adjusted to remain the same through the translation stage.

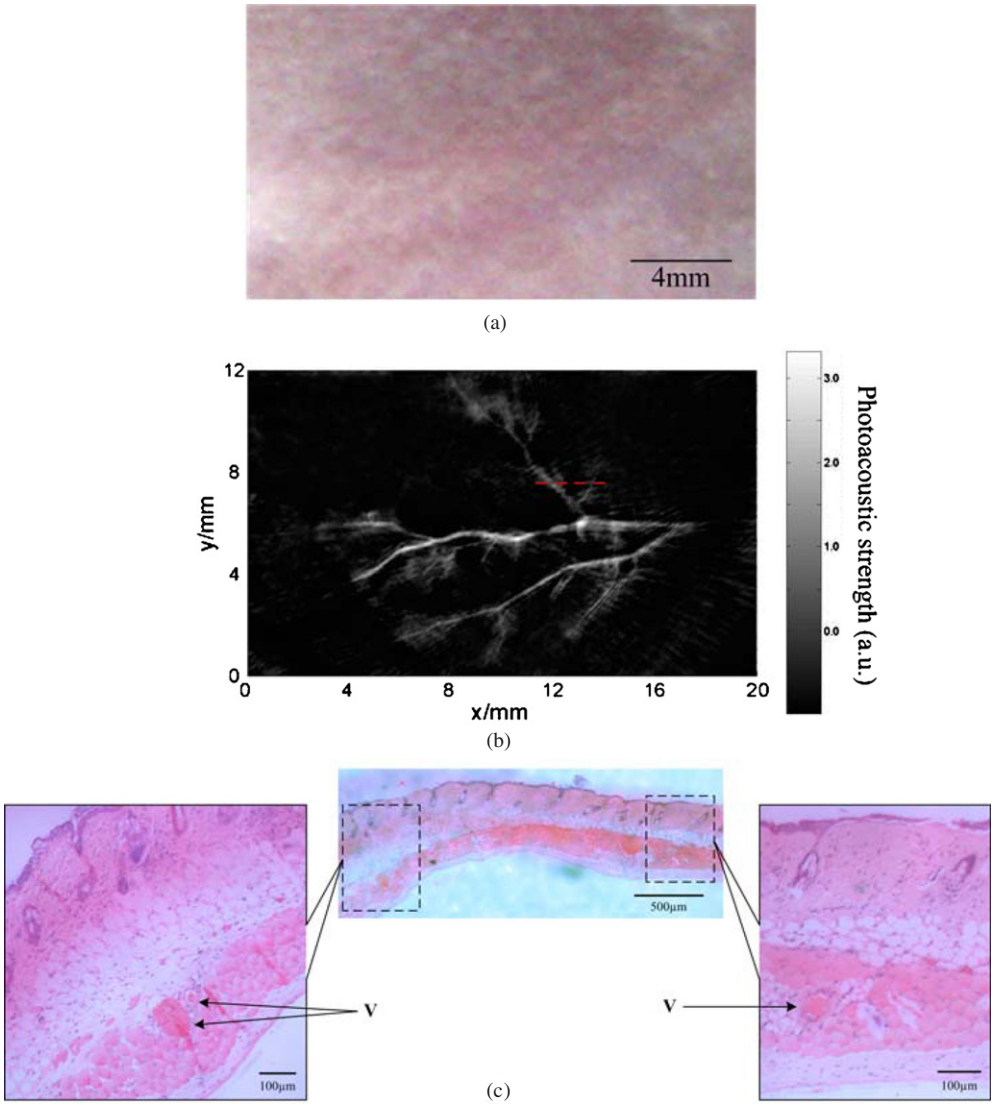

Figure 2. *In vivo* photoacoustic image of subcutaneous vasculature of the back of a mouse. (a) Photograph of the back of the mouse. (b) Photoacoustic image of subcutaneous vasculature of the back of the mouse. (c) HE stained histological section of the subcutaneous vasculature at the location marked with a (red) dashed line in (b). v: blood vessels.

3. Results and discussions

3.1. Photoacoustic image of subcutaneous vasculature

The spatial resolution of our photoacoustic imaging system is estimated to reach 80 μm (Xu and Wang 2003, Lao *et al* 2008). Figure 2 presents the photoacoustic image of the back of a living mouse. In a comparison of the photograph with the image, the subcutaneous vasculature of the back of the mouse is clearly shown in the photoacoustic image in figure 2(b),

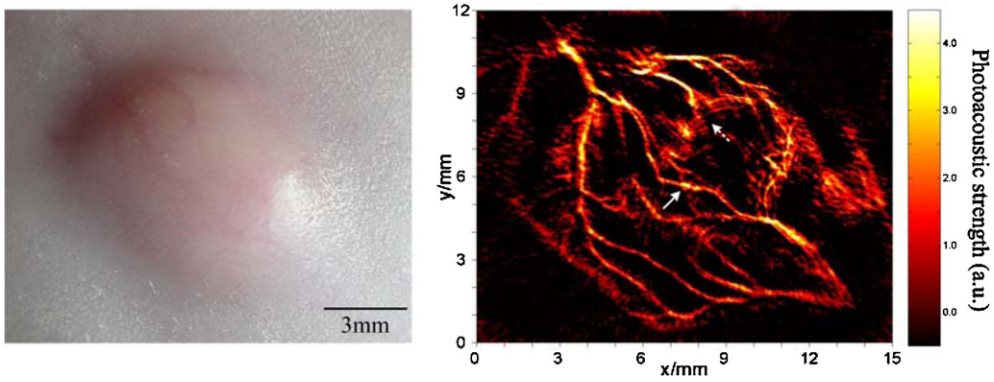

(a) (b)

Figure 3. *In vivo* photoacoustic image of vasculature in tumor region on the back of a mouse. (a) The photograph of the tumor nodule on the back of the mouse. (b) The photoacoustic image of vasculature in tumor region of the back of the mouse.

whereas only two main blood vessels are indistinctly visible to the naked eyes in figure 2(a). Up to four orders of vessel branching are observed in the photoacoustic image; also the trend of imaged blood vessels is obvious. The brighter colors indicate the higher strength of photoacoustic signals, i.e. stronger absorbed optical energy density. In order to demonstrate that the imaged blood vessels do exist at the location where no blood vessels are visible to the naked eyes from the photograph, a histological section was used to validate the accuracy of our photoacoustic imaging system. Figure 2(c) shows the hematoxylin-and-eosin (HE) stained histological section of subcutaneous vasculature at the location marked with a red dashed line in the photoacoustic image. The middle photograph displays a general picture of the mouse skin, and the photographs on both sides are the close-ups of two parts of the skin. Three blood vessels are easily distinguished in the close-ups. More importantly, the x–y plane position of these blood vessels matches that in the photoacoustic image well. The average depth of these blood vessels is ∼0.4 mm from the detected skin surface. It can be concluded that our photoacoustic imaging system is capable of imaging subcutaneous vasculature *in vivo* with high spatial resolution and accuracy.

3.2. Photoacoustic image of vasculature in tumor region

The morphological characteristics of tumor vasculature, such as vessel branching patterns, diameters and density, are different from those of normal vasculature. Tumor vasculature is highly disorganized, and vessels are tortuous and dilated, with uneven diameters, excessive branching and shunts (Carmeliet and Jain 2000). Figure 3(a) is the photograph of a tumor nodule on the back of a mouse 4 weeks after the tumor inoculation. The visual appearance of the tumor nodule is in oval shape, protruded over the skin surface ∼4 mm. The photoacoustic image, after the pseudo-color processing, is shown in figure 3(b). As can be seen from the image, vascular networks in the tumor region are clearly resolved; furthermore, the morphological characteristics of some blood vessels displayed in the photoacoustic image are similar to those of tumor vessels (Less *et al* 1991, Delorme and Knopp 1998). It is highly probable that this variation in the morphological characteristics of the vasculature is related to tumor angiogenesis. Firstly, a blood vessel with a dilated segment in a single branch is

found in the tumor region (indicated by the white solid-line arrow). Secondly, some blood vessels are highly tortuous compared with the normal vessel (indicated by the white dashed-line arrow) and have a trend of forming the vascular rings. Thirdly, the vessel density is significantly increased in tumor region compared to the normal vasculature in figure 2(b). From these results, our photoacoustic imaging system has demonstrated great potential to monitor developing vasculature during early tumor growth.

3.3. Photoacoustic images of neovascularization in early tumor growth

Both the visual appearance and the photoacoustic images of the inoculation site between 5 and 20 days after the inoculation, over a 5 day interval, are presented in figure 4. As for the visual appearance of the inoculation site, on day 5 there is a small protuberant mass on the skin and the subcutaneous vasculature is distinct to the naked eyes. From day 10 to day 20, hardly any blood vessels are visible in the inoculation site and the small protuberant mass gradually grows into a tumor nodule; the diameter and the protuberant height, measured by vernier calipers on day 20, are 8 mm and 3.5 mm, respectively.

The vasculature developing during early tumor growth is clearly revealed by the serial photoacoustic images. The gray scaling in all the photoacoustic images refers to the same range of absolute signal strength. Hence, after the pseudo-color processing, color differences displayed in the photoacoustic images represent real changes in the photoacoustic signal strength. The subcutaneous vasculature, which can be observed in the photoacoustic image on day 5, is in good agreement with that in the photograph. Also the vascular plexus in the bottom-left part of the image is clearly shown. On day 10, the architecture of blood vessels gradually becomes abnormal: some blood vessels are faded in the upper part of the image and the vascular plexus in the bottom-left is disturbed. The degree of disorder of the vascular anatomy on day 15 is higher than that on day 10, and the signal strength of the vascular plexus in the bottom-left is remarkably enhanced. Meanwhile, the vessel density has increased in the tumor region. On day 20, a significant change has occurred with the vasculature in the tumor region. Several dilated blood vessels with enhanced photoacoustic signal strength as well as highly disorganized vascular architecture are shown in the photoacoustic image. The structure of the vascular plexus in the bottom-left part of the image is totally different compared to that on day 5. Moreover, the vessel density has further increased, especially in the right part of the image.

3.4. Qualitative analysis of the developing vasculature

For the sake of giving qualitative analysis to morphology parameters of the developing vasculature during early tumor growth, an area of 6 mm $\times$ 9 mm contained in the white dashed-line rectangle was selected in all the photoacoustic images to assess tumor neovascularization. Parameters that reflected the morphological features of vasculature in tumor region were evaluated qualitatively in order to indicate the potential of photoacoustic imaging in monitoring the progress of tumor angiogenesis and anti-angiogenic therapy. Four blood vessels were selected randomly as samples and marked by a white dashed line in every photoacoustic image. The profiles along the white dashed lines of the images were then obtained for qualitative statistical analysis. According to the statistical results in the 20 day period, the average photoacoustic signal strength of blood vessels is in the rising trend during early tumor growth (figure 5); also the average vessel diameter is increased (figure 6). And an increase in the vessel density is obvious in the selected area every 5 days.

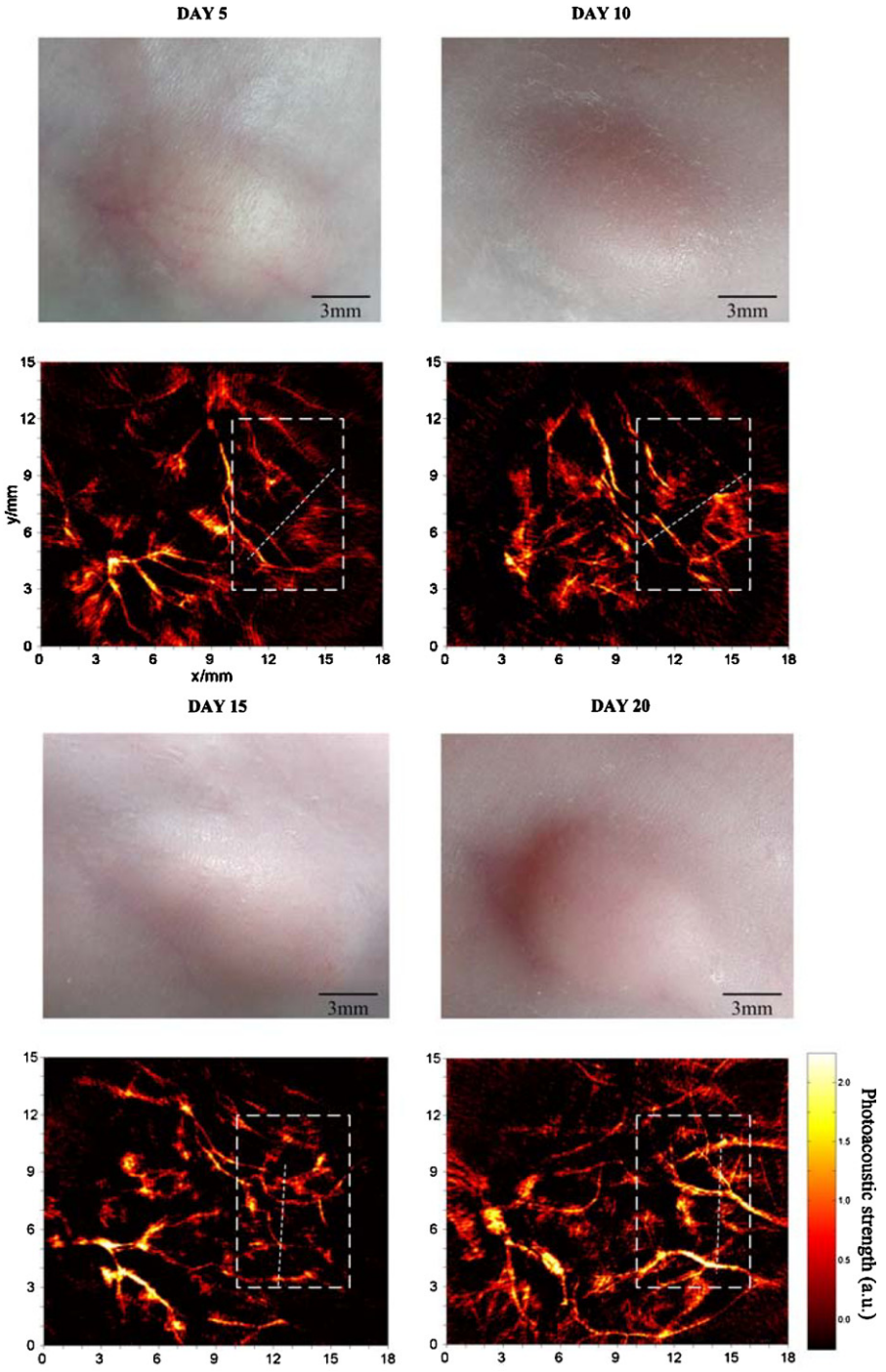

Figure 4. Photoacoustic images of neovascularization in tumor growth over a 20 day period.

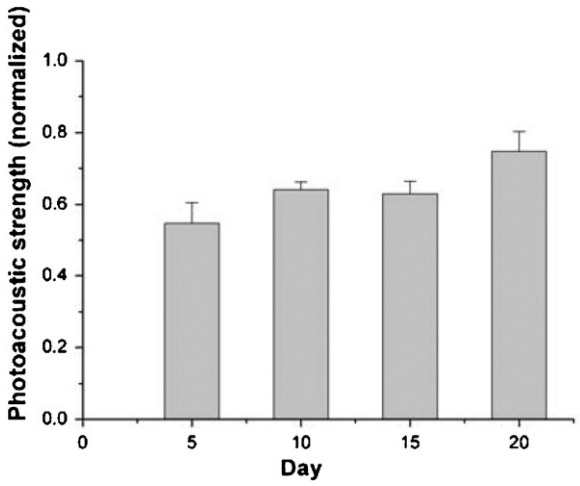

Figure 5. The statistical result of the average photoacoustic signal strength of blood vessels in tumor region during early tumor growth.

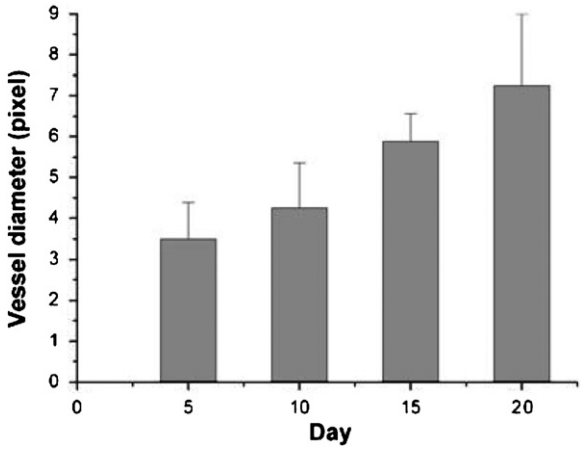

Figure 6. The statistical result of the average vessel diameter in tumor region during early tumor growth.

The enhancement of the photoacoustic signal strength of blood vessels is highly correlated with the increase of absorbed optical energy density. Hemoglobin is the main optical absorber in blood at a wavelength of 532 nm (Jacques and Prahl 2004). Based on this fact, one main reason for the enhancement of photoacoustic signal strength is that the total hemoglobin concentration in the tumor region is higher than that in the normal tissue (Zhu *et al* 2005). It is highly probable that tumor angiogenesis causes the increase of total average hemoglobin concentration. That blood vessels are dilated with uneven diameter, which is one of the abnormal morphological features in tumor-associated vasculature in contrast to normal vasculature, is clearly reflected both in the photoacoustic images and in the qualitative statistical analysis. The crescent average vessel diameter strongly predicts that the architecture of vasculature in tumor region gradually becomes chaotic and variable (Carmeliet and Jain

2000, Less *et al* 1991). Vessel density is a highly significant prognostic indicator in early stage tumors (Weidner *et al* 1992). The increase of vessel density in the tumor region, revealed by the photoacoustic images, demonstrates that the tumor has greater density than normal tissue (Hulka *et al* 1995).

Although the higher total hemoglobin concentration is the main reason for the enhancement of photoacoustic signal strength, some other factors, such as the physiological status of the mouse and the experimental environment, are also the cause of the change of photoacoustic signal strength. Thus in our experiments, the morphology parameters of the developing vasculature in tumor region could only be analyzed qualitatively from the statistical results, and could hardly perform a quantitative analysis. Since in our study a hydrophone is used to receive photoacoustic signals, the reconstructed image is the congruence of the photoacoustic signals in a special range of depth. Therefore, the depth information of early tumor growth is lost. In addition, our photoacoustic imaging system involves only a single transducer, and the total acquisition time is $\sim$18 min. So a fast multi-element phase-controlled photoacoustic imaging system is needed to achieve real-time three-dimensional imaging in the future (Yang *et al* 2005, 2006, 2007a, 2007b, 2007c). The current study was performed with a single wavelength using the endogenous contrast provided by blood. The next step of our work is to acquire some functional parameters, such as the oxygenated and deoxygenated hemoglobin distribution, by the use of several characteristic absorption wavelengths (Zhang *et al* 2006). Furthermore, molecular photoacoustic imaging with exogenous contrast agents will bring us closer to the clinical application of this technique for early tumor detection and treatment monitoring.

4. Conclusions

We have demonstrated that photoacoustic imaging is a noninvasive effective imaging modality for monitoring the progress of vasculature during early tumor growth with high resolution and good contrast. Not only the morphological features of vasculature in tumor region are clearly revealed, but also further information, including changes in morphology and optical absorption of blood vessels, is directly shown in the qualitative statistical analysis. These results prove that photoacoustic imaging has the potential to become a useful tool in detecting early stage tumor and monitoring the progress of anti-angiogenic therapy.

Acknowledgments

We thank Huiying Wang for supplying us with the tumor cells and the assistance in experiments from Feifan Zhou and Yujun Wu. This research is supported by the National Natural Science Foundation of China (30470494; 30627003) and the Natural Science Foundation of Guangdong Province (7117865).

References

Anderson H, Price P, Blomley M, Leach M O and Workman P 2001 Measuring changes in human tumor vasculature in response to therapy using functional imaging techniques *Brit. J. Cancer* **85** 1085–93

Carmeliet P and Jain R K 2000 Angiogenesis in cancer and other diseases *Nature* **407** 249–57

Delorme S and Knopp M V 1998 Non-invasive vascular imaging: assessing tumour vascularity *Eur. Radiol.* **8** 517–27

Ermilov S A, Conjusteau A, Mehta K, Lacewell R, Henrichs P M and Oraevsky A A 2006 128-channel laser optoacoustic imaging system (LOIS-128) for breast cancer diagnostics *Proc. SPIE* **6086** 608609

Hulka C A, Smith B L, Sgroi D C, Tan L, Edmister W B, Semple J P, Campbell T, Kopans D B, Brady T J and Weisskoff R M 1995 Benign and malignant breast lesions: differentiation with echo-planar MR imaging *Radiology* **197** 33–8

Jacques S L and Prahl S A 2004 *Absorption Spectra for Biological Tissues* (Portland, OR: Oregon Medical Laser Center)

Khamapirad T, Henrichs P M, Mehta K, Miller T G, Yee A T and Oraevsky A A 2005 Diagnostic imaging of breast cancer with LOIS: clinical feasibility *Proc. SPIE* **5697** 35–44

Krix M, Kiessling F, Vosseler S, Farhan N, Mueller M M, Bohlen P, Fusenig N E and Delorme S 2003 Sensitive noninvasive monitoring of tumor perfusion during antiangiogenic therapy by intermittent bolus-contrast power Doppler sonography *Cancer Res.* **63** 8264–70

Ku G, Wang X D, Xie X Y, Stoica G and Wang L V 2005 Imaging of tumor angiogenesis in rat brains *in vivo* by photoacoustic tomography *Appl. Opt.* **44** 770–5

Lao Y Q, Zhou F F and Wang H Y 2008 *In vivo* photoacoustic imaging of subcutaneous vasculature and vascular anomalies in small animals *Eur. Phys. J. Appl. Phys.* **41** 151–5

Less J R, Skalak T C, Sevick E M and Jain R K 1991 Microvascular architecture in a mammary carcinoma: branching patterns and vessel dimensions *Cancer Res.* **51** 265–73

Siphanto R I, Thumma K K, Kolkman R G M, van Leeuwen T G, de Mul F F M, van Neck J W, van Adrichem L N A and Steenbergen W 2005 Serial noninvasive photoacoustic imaging of neovascularization in tumor angiogenesis *Opt. Express* **13** 89–95

Wang Y, Xing D, Zeng Y G and Chen Q 2004 Photoacoustic imaging with deconvolution algorithm *Phys. Med. Biol.* **49** 3117–24

Weidner N, Folkman J, Pozza F, Bevilacqua P, Allred E N, Moore D H, Meli S and Gasparini G 1992 Tumor angiogenesis: a new significant and independent prognostic indicator in early-stage breast carcinoma *J. Natl Cancer Inst.* **84** 1875–87

Xiang L Z, Xing D, Gu H M, Yang D W, Yang S H, Zeng L M and Chen W R 2007 Real-time optoacoustic monitoring of vascular damage during photodynamic therapy treatment of tumor *J. Biomed. Opt.* **12** 014001

Xu M H and Wang L V 2003 Analytic explanation of spatial resolution related to bandwidth and detector aperture size in thermoacoustic or photoacoustic reconstruction *Phys. Rev.* E **67** 056605

Yang D W, Xing D, Gu H M, Tan Y and Zeng L M 2005 Fast multi-element phase-controlled photoacoustic imaging based on limited-field filtered back projection algorithm *Appl. Phys. Lett.* **87** 194101

Yang D W, Xing D, Tan Y, Gu H M and Yang S H 2006 Integrative prototype B-scan photoacoustic tomography system based on a novel hybridized scanning head *Appl. Phys. Lett.* **88** 174101

Yang D W, Xing D, Yang S H and Xiang L Z 2007a Fast full-view photoacoustic imaging by combined scanning with a linear transducer array *Opt. Express* **15** 15566–75

Yang S H, Xing D, Lao Y Q, Yang D W, Zeng L M, Xiang L Z and Chen W R 2007b Noninvasive monitoring of traumatic brain injury and post-traumatic rehabilitation with laser-induced photoacoustic imaging *Appl. Phys. Lett.* **90** 243902

Yang S H, Xing D, Zhou Q, Xiang L Z and Lao Y Q 2007c Functional imaging of cerebrovascular activities in small animals using high-resolution photoacoustic tomography *Med. Phys.* **34** 3294–301

Zhang H F, Maslov K, Stoica G and Wang L V 2006 Functional photoacoustic microscopy for high-resolution and noninvasive *in vivo* imaging *Nat. Biotechnol.* **24** 848–51

Zhu Q, Cronin E B, Currier A A, Vine H S, Huang M M, Chen N G and Xu C 2005 Benign versus malignant breast masses: optical differentiation with US-guided optical imaging reconstruction *Radiology* **237** 57–66

Zhu Q, Huang M M, Chen N G, Zarfos K, Jagjivan B, Kane M, Hedge P and Kurtzman S H 2003 Ultrasound-guided optical tomographic imaging of malignant and benign breast lesions: initial clinical results of 19 cases *Neoplasia* **5** 379–88